

---

# STBLLM: Breaking the 1-Bit Barrier with Structured Binary LLMs

---

Peijie Dong<sup>1†</sup>, Lujun Li<sup>2†</sup>, Dayou Du<sup>1</sup>, Yuhan Chen<sup>1</sup>, Zhenheng Tang<sup>1,3</sup>, Qiang Wang<sup>4</sup>,  
 Wei Xue<sup>2</sup>, Wenhan Luo<sup>2</sup>, Qifeng Liu<sup>1</sup>, Yike Guo<sup>2\*</sup>, Xiaowen Chu<sup>1\*</sup>  
<sup>1</sup>HKUST(GZ) <sup>2</sup>HKUST <sup>3</sup>HKBU <sup>4</sup>HIT(SZ)

pdong212@connect.hkust-gz.edu.cn, lilujunai@gmail.com, {yikeguo, xwchu}@ust.hk\*

## Abstract

In this paper, we present STBLLM, the first structural binarization framework for compressing Large Language Models (LLMs) to less than 1-bit precision. LLMs have achieved remarkable performance, but their heavy memory requirements have hindered widespread adoption, particularly on resource-constrained devices. Binarization, which quantifies weights to a mere 1-bit, achieves a milestone in increasing computational efficiency. However, we observe that some weights in binarized LLMs can be randomly flipped without significant performance degradation, indicating the potential for further compression. To exploit this, our STBLLM employs an N:M sparsity to perform structural binarization of the weights. First, we introduce a new Standardized Importance (SI) metric that considers weight magnitude and input feature norm to better evaluate weight significance. Then, we propose a layer-wise approach where different layers of the LLM can be sparsified with varying N:M ratios, balancing compression and accuracy. Finally, we use residual approximation with double binarization to preserve information for salient weights. In addition, we utilize a fine-grained grouping strategy for less important weights that applies different quantization schemes to sparse, intermediate, and dense regions. We conduct extensive experiments on various language models, including the LLaMA-1/2/3, OPT family, and Mistral, to evaluate the effectiveness of STBLLM. The results demonstrate that our approach performs better than other compressed binarization LLM methods while significantly reducing memory requirements. Code will be released upon acceptance.

## 1 Introduction

The advent of large language models (LLMs), such as [1–3], has revolutionized the field of natural language processing (NLP) [4]. These powerful models exhibit remarkable performance, rivaling and even surpassing human capabilities in certain domains [5, 6]. However, the immense scale and complexity of LLMs present significant challenges in terms of memory requirements [7, 8], hindering their widespread deployment, especially in resource-constrained environments. For instance, OpenAI’s GPT-3 model, with its 175 billion parameters, required immense energy consumption during the training and inference process [9]. To address this issue, model compression techniques, such as quantization [10], pruning [11], distillation [12], and low-rank decomposition [13], have gained increasing attention in reducing the computational footprint of LLMs while preserving their performance. One promising approach is network binarization, the most aggressive quantization method. Binarization quantizes original floating-point weights with binary values (−1 or +1), significantly reduces memory storage, and enables efficient binary arithmetic operations on various hardware platforms.

---

\*Corresponding authors, † equal contribution. Work in progress, revisions ongoing.

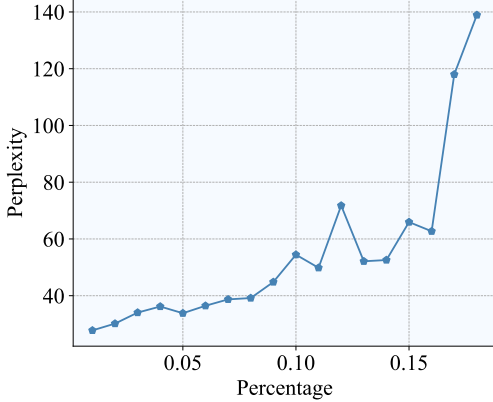


Figure 1: **The impact of randomly flipping non-salient binarized weights on perplexity in a 1-bit LLaMA-2-7B.** The x-axis represents the percentage of binarized weights flipped from -1 to 1 or vice versa. Even in a highly quantized 1-bit LLM, there is some redundancy present.

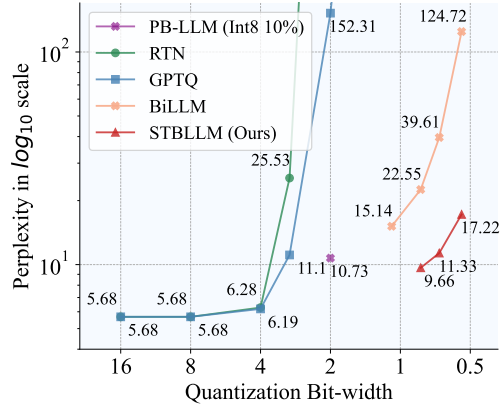


Figure 2: **The perplexity of LLaMA-1-13B on the Wikitext2 under different bit-widths.** RTN and GPTQ show a drastic performance drop at ultra-low bit-widths. Our proposed STBLLM achieves higher performance compared to BiLLM at sub 1-bit widths.

Pioneering binarization methods [14, 15] present customized binary structures and training paradigms for binarized neural networks (BNNs) in vision tasks. Building upon these foundational approaches, subsequent methods [16–22] have advanced the field by integrating sparse kernel techniques [17, 18] and pruning methodologies [19, 21, 22]. These innovations serve to further optimize model compression

For language models, inspired by the success of 4-bit and 8-bit quantization methods, some studies [23–25] continue to explore ultra-low-bit or even 1-bit precision. For example, the post-training method PB-LLM [25] partially binarizes LLMs with an optimal scaling factor strategy, preserving a small subset of the higher bit-precision weights. BiLLM [23] proposes a residual approximation strategy to improve 1-bit LLMs. While these methods represent the most aggressive quantization approaches, it is crucial to consider that popular floating-point LLMs already contain model sizes ranging from 7 billion to 140 billion parameters. As a result, 1-bit LLMs still need to be further accelerated and optimized for many resource-constrained devices and real-time scenarios. This naturally raises a key question: *Is there any compression method with less than 1-bit weight representation that can further push the quantization of LLMs?*

For this question, two key observations inspire us: **(1) Not all weights contribute equally to the performance of 1-bit LLMs.** As shown in Figure 1, performing randomly weight flipping for non-salient weights results in only a minimal performance drop. These findings indicate that even in highly quantized 1-bit LLMs, a subset of redundant weights exists that can be further compressed without substantially impacting the overall performance of LLMs. This observation suggests the potential for further compression by selectively encoding the most significant weights while discarding or compressing the less important ones. **(2) Structured sparsity techniques,** such as N:M sparsity methods [26–28], leverage the inherent structure and patterns in the weight distribution, allowing for more efficient compression. N:M sparsity indicates that each bank has M continuous weights, and only N elements are kept after pruning. These N:M sparsity methods have good hardware-accelerated support in recent LLM pruning models [29, 30], enabling efficient deployment on various platforms [31]. However, traditional binarization techniques [14] often treat weights as independent entities, failing to exploit the inherent structure and patterns in the weight matrices. This oversight leads to sub-optimal compression and inefficient utilization of available resources. These observations encourage us to explore N:M sparsity tailored specifically for 1-bit LLMs to achieve further speedups and compression gains.

Based on these observations, we develop our STBLLM approach, **ST**ructured **B**inarization for **LLM**s to achieve extreme compression ratios while mitigating performance degradation. Our workflow first applies the metric-based sparsity, then performs the adaptive N:M binarization, and finally applies block-wise error compensation to improve the performance further. In particular, to measure the importance of weights, we introduce a Standardized Importance (SI) metric that addresses the

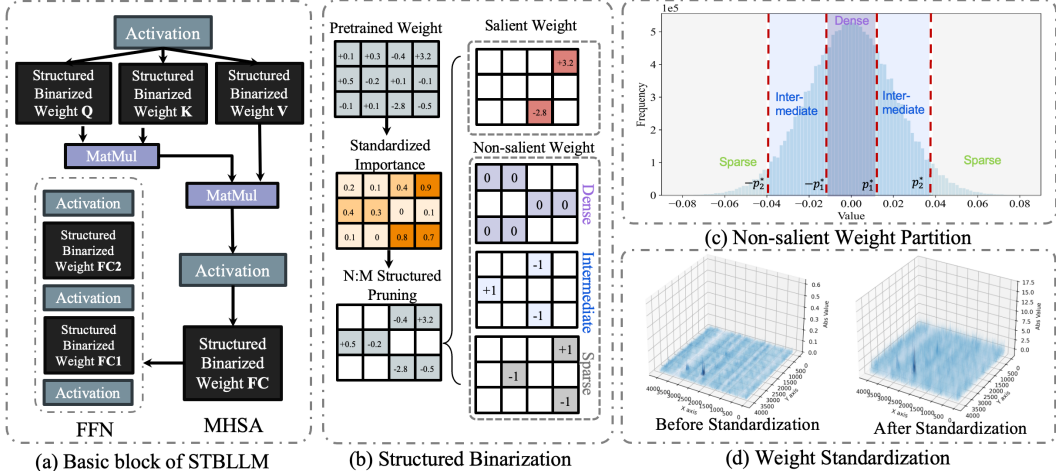


Figure 3: (a) PTQ framework in Structured Binarized LLM (STBLLM). We apply structured binarization to all of the weights. (b) Structured Binarized Weight Computation Procedure. We first perform N:M structure pruning to pre-trained weight (here  $N=2$ ,  $M=4$ ), then perform binarization by assign weight to salient and non-salient one. (c) Trisection partition for Symmetric Gaussian Distribution of Non-salient Weight. (d) Illustration of Weight Standardization on LLaMA-2-7B.

issues of extreme weight values and computationally expensive Hessian-based methods used in prior work. Our SI metric evaluates weight importance by considering both the weight magnitude and the corresponding input feature norm, providing a more holistic assessment of a weight’s significance. We then propose an adaptive layer-wise structured binarization approach, where different layers of the LLM can be sparsified with varying N:M ratios to balance compression and accuracy. We employ a residual approximation technique for the salient weight parameters that combines double binarization to preserve the critical information. For the non-salient weight parameters, we utilize a fine-grained grouping strategy based on a trisection search algorithm to find optimal breakpoints and apply different quantization schemes to the sparse, intermediate, and dense weight regions. By tailoring these structured representations specifically for 1-bit LLMs, we can unlock new avenues for model compression and optimization, enabling more widespread deployment of these powerful language models in resource-constrained environments.

To validate the effectiveness of STBLLM, we conduct extensive experiments on various language models, including the LLaMA-1/2/3 [2, 32], OPT [33] and Mistral [34]. As presented in Figure 2, our STBLLM achieve better trade-off between performance and bit-width. STBLLM with 0.8 bit can achieve lower perplexity compared with BiLLM with 1.1 bit. For language modeling on datasets, we observe that STBLLM significantly outperforms the state-of-the-art 1-bit quantization method BiLLM and other low-bit baselines like PB-LLM and GPTQ. Notably, on the challenging LLaMA-1-7B model, STBLLM achieves a perplexity of 31.72 at just 0.55 bits per weight, compared to 688.73 for BiLLM - an over  $20\times$  gain. Even at 65B parameters, our 0.55-bit STBLLM outperforms BiLLM’s 0.7-bit and PB-LLM’s 1.7-bit versions. We see similar trends across the OPT and Mistral model families. On zero-shot benchmarks spanning Winogrande [35], OpenBookQA [36], HellaSwag [37], and more, STBLLM retains significantly higher accuracy than BiLLM under 4:8 and 6:8 structured binarization settings across 13B and 30B LLaMA models. For example, on LLaMA-1-30B, our 0.55-bit STBLLM achieves 51.78% average accuracy versus just 43.72% for BiLLM. These results demonstrate STBLLM’s ability to push the frontiers of LLM compression to unprecedented sub-1-bit levels while maintaining competitive performance, paving the way for widespread deployment on resource-constrained environments.

## 2 Related Work

**Quantization and Binarization of LLMs.** Quantization reduces high-precision parameters to lower-bit representations, thereby decreasing storage and computation requirements. Recent research has effectively applied Quantization-Aware Training (QAT) and Post-Training Quantization (PTQ) to LLMs. QAT incorporates quantization during training, allowing the model to learn better represen-

tations for low-bit weights. LLM-QAT [38] self-generate data for data-free distillation. To further enhance performance, BitDistiller [39] employs asymmetric quantization and a novel distillation objective, while DB-LLM [40] splits its weights into two independent sets of binaries. However, retraining is often too costly and inefficient for LLMs with extensive parameters. On the other hand, PTQ is applied directly to pre-trained models without the need for additional training. Methods like GPTQ [41] and Quip [42] minimized block quantization errors in LLMs through second-order error compensation. Other approaches such as AWQ [43], OWQ [44], and SPQR [45] focus on prioritizing salient weights to maintain their information representation capacity. Without retraining, our work effectively manages the significant weights and optimizes scale values for less critical weights, advancing LLMs towards binarization quantization. Binarization, which constrains quantized parameters to a 1-bit representation, is the most extreme quantization method and has proven effective for vision tasks, as demonstrated by XNOR-Net [14] and Bi-Real Net [15]. Currently, several works are exploring the binarization of LLMs. BitNet [46] demonstrated effective scaling when training 1-bit weights of LLMs from scratch. PB-LLM [25] and Onebit [24] utilize QAT training with a Straight Through Estimator (STE) [47]. The current method, BiLLM [23], advances PTQ to binarization of LLMs by using Hessian-based metrics to select salient weights and a residual approximation for compensation. By identifying redundant information, we further reduce weights below 1-bit through PTQ, achieving shallow storage and improved accuracy.

**Sparsity Methods** remove entire structures, such as neurons, filters, or channels, from the neural network. LLM-Pruner [48] aims to identify the coupled structure in LLM and propose grouped importance estimation for pruning. SliceGPT [49] remove the rows and columns of weight to reduce parameters. Sheared LLaMA [50] propose targeted structure pruning to prune an LLM to a specified target shape by removing the number of heads, removing the layer, and reducing the dimension of the intermediate and hidden layers. Another prevalent existing structured pruning method is depth pruning, which means removing layers entirely from the pre-trained LLMs. Semi-structured sparsity combines the benefits of both structured and unstructured pruning methods. It removes weights in a manner that creates regular, predictable patterns like N:M but does not necessarily prune entire structures like filters or channels. This approach balances the fine-grained sparsity of unstructured pruning and the hardware-friendly structure of structured pruning. Most post-training pruning (PTP) methods support semi-structure pruning as the key to semi-structured pruning is also measuring the importance of each element. For example, SparseGPT [29] and Wanda [30] perform N:M pruning by evaluating the importance of M successive elements in the weight and only keeping the top-N elements of them. RIA [51] propose channel permutation to retain more essential elements within the weight under N:M sparsity. FLAP [52] apply adaptive structure search for performance compensation.

**Pruning and Sparsity in Binarized Networks.** Subsequent studies [16–22] have investigated the convergence of network binarization and pruning techniques to develop efficient and compact neural networks. These approaches seek to synergize the advantages of BNNs with sparsity-inducing methodologies to optimize model size and computational requirements while preserving performance. Si-BNN [16] implements activation quantization to either 0 or +1, thereby introducing sparsity into binary representation. BNN Pruning [21] orchestrates the pruning process in BNNs based on weight flipping frequency. STQ-Nets [22] integrates acceleration techniques from binary convolution algorithms through structured pruning. BAP [19] examines the efficacy of extremely sparse networks with binary connections via software-hardware codesign. Sparks [17] proposes sub-1-bit models by clustering kernels into sub-codebooks on convolution-based networks. While these studies demonstrate the increasing interest in combining binarization and pruning techniques, they predominantly focus on convolution-based architectures. In contrast to Convolutional Neural Networks, LLMs based on transformer architectures cannot undergo complete fine-tuning due to their extensive scale and parameter space. Our research represents the first attempt to apply pruning to binarization networks specifically for LLMs. Furthermore, transformer-based architectures lack 3x3 kernels, presenting challenges in the application of existing codebook-based methods.

### 3 Methodology

In this section, we introduce our STBLLM framework, as depicted in Figure 3. We employ structured binarization for all weights within the Feed-forward Network (FFN) and Multi-head Self-attention (MHSA) modules. Specifically, we introduce the concept of Standardized Importance (SI) to evaluate the saliency of each weight under N:M sparsity constraints (refer to the left part of Figure 3(b)).

---

**Algorithm 1** Framework of STBLLM: Details of each function are shown in Alg. 2

---

func StructuredBinaryLLM( $\mathbf{W}$ ,  $\mathbf{X}$ ,  $\beta$ ,  $\lambda$ )**Input:**  $\mathbf{W} \in \mathbb{R}^{n \times m}$  denotes weight matrix;  $\mathbf{X} \in \mathbb{R}^{r \times d}$  represents calibration data;  
 $\beta$  denotes block size;  $\lambda$  represents hessian regularizer**Output:**  $\mathbf{B}$  - structured binarized weights

- 1:  $\mathbf{H} := 2\mathbf{X}\mathbf{X}^\top$  //  $\ell^2$  error hessian matrix
  - 2:  $\mathbf{H}^c := \text{Cholesky}((\mathbf{H} + \lambda\mathbf{I})^{-1})$
  - 3:  $\mathbf{B} := 0_{n \times m}$
  - 4: **for**  $b = 0, \beta, 2\beta, \dots, N$  **do**
  - 5:    $\mathbf{W}^{si} := \text{Standardized\_Importance}(\mathbf{W}_{:,b:b+\beta})$
  - 6:    $\mathbf{W}^s := \text{Semi-Structured}(\mathbf{W}_{:,b:b+\beta}^{si}, \mathbf{W}_{:,b:b+\beta})$
  - 7:    $\text{row}_s\{\cdot\} := \text{Salient}(\mathbf{W}_{:,b:b+\beta}, \mathbf{H}^c)$
  - 8:    $\tilde{\mathbf{B}}_1 := \text{Res\_Approx}(\mathbf{W}_{:,j \in \{\text{row}_s\}}^s)$
  - 9:    $p_1^*, p_2^* := \text{NonSalientAwareQuant}(\mathbf{W}_{i,j \notin \{\text{row}_s\}}^s)$
  - 10:    $\tilde{\mathbf{B}}_2, \tilde{\mathbf{B}}_3, \tilde{\mathbf{B}}_4 := \text{Trisection}(\mathbf{W}_{|w_{i,j}|}, p_1^*, p_2^*)$
  - 11:    $\mathbf{B}_{:,b:b+\beta} := \tilde{\mathbf{B}}_1 \cup \tilde{\mathbf{B}}_2 \cup \tilde{\mathbf{B}}_3 \cup \tilde{\mathbf{B}}_4$
  - 12:    $\mathbf{E} := (\mathbf{W}_{:,b:b+\beta} - \mathbf{B}_{:,b:b+\beta}) / \mathbf{H}_{bb:b+b\beta}^c$
  - 13:    $\mathbf{W}_{:,b+\beta} := \mathbf{W}_{:,b+\beta} - \mathbf{E} \cdot \mathbf{H}_{b:b+\beta,b+b\beta}^c$  // block-wise OBC
  - 14: **end for**
  - 15: **Return**  $\mathbf{B}$
- 

For the binarization process, we leverage the Hessian matrix to distinguish between salient and non-salient weights. Salient weights are handled using residual approximation, following the methodology outlined in BiLLM [23]. For non-salient weights, we propose a Non-salient Aware Quantization technique, which further divides these weights into Dense, Intermediate, and Sparse regions (as shown in the right part of Figure 3(c)). To optimally partition the non-salient weights into three distinct regions, we utilize a trisection search strategy to determine the appropriate  $p_1^*$  and  $p_2^*$  values. In the subsequent update step, we apply block-wise error compensation [29, 41] to preserve performance following post-training quantization (PTQ). Alg. 1 provides a comprehensive overview of the STBLLM process, with detailed implementation steps available in Appendix A.

### 3.1 Preliminaries

**Binarization.** Binarized compression seeks to quantize floating-point (FP) weights, represented as  $\mathbf{W}_{FP}$ , into 1-bit values (i.e.,  $\pm 1$ ). During forward propagation, the sign function is used to binarize the original parameter tensor:

$$\mathbf{B} := \alpha \cdot \text{sign}(\mathbf{W}_{FP}), \quad (1)$$

$$\text{sign}(w) := \begin{cases} 1 & \text{if } w \geq 0, \\ -1 & \text{others,} \end{cases} \quad (2)$$

where  $\mathbf{W}_{FP} \in \mathbb{R}^{n \times m}$  is the 32-bit floating-point weight, and  $\mathbf{B} \in \mathbb{R}^{n \times m}$  is the binarized output, and  $\alpha := \frac{\|\mathbf{W}\|_{l_1}}{m}$ . The parameter  $n$  and  $m$  represent the size of the weight matrix. The scaling factor  $\alpha \in \mathbb{R}^n$  is applied in a channel-wise manner [14].

**N:M Sparsity.** Inspired by the experiments shown in Figure 1, we observe the binarized the redundancy in LLMs. By applying the N:M binarization for LLMs, we can achieve an extreme compression ratio of less than 1-bit. Specifically, we propose a novel N:M sparsity method that encodes N consecutive non-zero elements in the weight matrix with a single M-bit codeword.

However, it would cause performance degradation. To alleviate this problem, we propose several techniques from different perspectives: (1) Importance Measurement. Previous methods [41, 53, 23] utilize Hessian-based methods to measure the importance, but these methods can be computationally expensive and may not capture the true importance of parameters in LLMs. (2) Layer-wise Assignment. Previous PTP methods [29, 51] utilize the uniform sparsity ratio among different layers. However, recently, evidence [54] shows that not all layers have the same redundant level, thus non-uniform sampling can help retain the performance. (3) Hierarchical Quantization. Previous PTQ methods for LLM like AWQ [43], OWQ [55] and BiLLM [23] split the weights into salient and



non-salient parameters using the magnitude of activation or Hessian matrix. They mainly focus on salient weights, as most researchers believe they contribute to the final performance. However, the non-salient parameters also play an essential role in quantization.

### 3.2 Standardized Importance Metric

Many previous works, such as DB-LLM [53], SparseGPT [29], GPTQ [41], and BiLLM [23], utilize the Hessian metric to measure the importance of weights. However, we observe that the presence of extreme values in the weights have significant impact on Hessian computation (See Appendix C). To address this issue, we present a Standardized Importance (SI) metric. The computation of SI does not involve the second-order information of the weights, which can be computationally expensive for LLMs. Specifically, we employ standardization to mitigate the issue of extreme values in weights by transforming the weights to have a mean of zero and a standard deviation of one. This process ensures that all weights are on a similar scale, reducing the disproportionate influence of extreme values on the Hessian matrix. For a linear layer with weight  $\mathbf{W} \in \mathbb{R}^{n \times m}$ , which takes in input activation  $\mathbf{X} \in \mathbb{R}^{r \times d}$ , where  $r$  is the batch size and  $d = m$  is the input dimension. We propose to evaluate the importance of each weight by the product of its magnitude and the corresponding input feature norm. The score for the current weight  $\mathbf{W}_{i,j}$  is defined as:

$$\mathbf{S}_{i,j} = \sigma(\mu(|\mathbf{W}_{i,j}|)) \cdot \|\mathbf{X}_{:,j}\|_2, \quad \sigma(\hat{w}) = \frac{w - \mu_{\mathbf{W}}}{\sigma_{\mathbf{W}}}, \quad \mu(|\mathbf{W}_{i,j}|) = \frac{|\mathbf{W}_{i,j}|}{\sum_j |\mathbf{W}_{i,j}|} + \frac{|\mathbf{W}_{i,j}|}{\sum_i |\mathbf{W}_{i,j}|}, \quad (3)$$

where  $\sigma(\cdot)$  is a normalization function that standardizes the weight magnitude  $\mu(|\mathbf{W}_{i,j}|)$  using the mean  $\mu_{\mathbf{W}}$  and standard deviation  $\sigma_{\mathbf{W}}$  of all weights in the layer. The weight magnitude  $\mu(|\mathbf{W}_{i,j}|)$  is computed as the sum of the L1-normalized magnitude across the input dimension  $j$  and the output dimension  $i$ . The input feature norm  $\|\mathbf{X}_{:,j}\|_2$  is calculated as the L2 norm of the  $j$ -th column input activation  $\mathbf{X}$ . By multiplying the standardized weight magnitude  $\sigma(\mu(|\mathbf{W}_{i,j}|))$  with the input feature norm  $\|\mathbf{X}_{:,j}\|_2$ , the importance score  $\mathbf{S}_{i,j}$  takes into account both the significance of the weight itself and the activation level of the associated input feature. To prune the linear layer, we rank all the weights based on their importance scores  $\mathbf{S}_{i,j}$  and remove a specified percentage of the weights with the lowest scores. This pruning strategy aims to preserve the most significant weights contributing to the layer’s output while eliminating less important weights to reduce the model’s size and computational complexity.

### 3.3 Adaptive Layer-wise Binarization

**N:M Binary Weight Vector.** To achieve compression beyond standard binarization, we propose an N:M sparsity approach, where M binary values are represented by N values ( $N < M$ ). This allows for further compression while preserving the salient information in the weight tensors. Specifically, we employ the mixed N:8 sparsity configuration following DominoSearch [56].

**Layer-wise N:M Assignment.** To achieve better accuracy-efficiency trade-offs, we introduce adaptive layer-wise structured binarization, where different layers of the LLM can be sparsified with different N:M ratios. (For example, with a target ratio of 4:8, layers can have ratios like 3:8, 4:8, and 5:8 while maintaining the overall 4:8 ratio.) This flexibility allows for more aggressive compression in less important layers while preserving higher precision in crucial layers.

The layer-wise N:M ratios are assigned based on the relative importance of each layer, measured by the L2 norm of its weight parameters. Let  $\omega_i$  and  $\omega_{\text{total}}$  be the L2 norm of layer  $i$  and the sum across all layers, respectively. The relative importance  $\alpha_i$  of layer  $i$  is  $\alpha_i = \frac{\omega_i}{\omega_{\text{total}}}$ . The N:M ratio for layer  $i$  is  $\frac{N_i}{M_i} = \alpha_i + (1 - \alpha_i) \cdot R_{\text{target}}$ , where  $R_{\text{target}}$  is the target overall compression ratio. More important layers have higher N:M ratios (less sparsification), approaching 1:1 for the most important ones. Less important layers have lower N:M ratios, approaching  $R_{\text{target}}$  for the least important ones. This ensures the overall compression ratio meets  $R_{\text{target}}$ .

### 3.4 Non-salient Aware Quantization

Based on the observations that a small fraction of salient weights is critical to the LLM quantization [43, 57], we split the weights into the salient and non-salient parts and then apply a higher bit for salient one and lower-bit for non-salient one, as:

Table 1: Average bit results from structural searching and residual binarization of OPT, LLaMA-1, and LLaMA-2 families. \*OPT-66B, LLaMA-1-65B and LLaMA-2-70B.

Model	BiLLM				BiLLM-4:8				BiLLM-5:8				BiLLM-6:8			
	7B	13B	30B	65-70B*	7B	13B	30B	65-70B*	7B	13B	30B	65-70B*	7B	13B	30B	65-70B*
OPT	1.10	1.12	1.12	1.13	0.55	0.56	0.56	0.56	0.69	0.70	0.70	0.71	0.83	0.84	0.84	0.85
LLaMA-1	1.09	1.09	1.10	1.10	0.54	0.54	0.55	0.55	0.68	0.68	0.69	0.69	0.82	0.82	0.83	0.83
LLaMA-2	1.07	1.08	N/A	1.09	0.53	0.54	N/A	0.54	0.67	0.67	N/A	0.68	0.80	0.81	N/A	0.82

**Salient Part:** In our cases, for salient weight, we apply residual approximation [23], which is composed of double binarization weight, as follows:

$$\begin{cases} \alpha_o^*, \mathbf{B}_o^* = \arg \min_{\alpha_o, \mathbf{B}_o} \|\mathbf{W} - \alpha_o \mathbf{B}_o\|^2, \\ \alpha_r^*, \mathbf{B}_r^* = \arg \min_{\alpha_r, \mathbf{B}_r} \|(\mathbf{W} - \alpha_o^* \mathbf{B}_o^*) - \alpha_r \mathbf{B}_r\|^2, \end{cases} \quad (4)$$

where  $\mathbf{B}_o$  denotes the original binary tensor, and  $\mathbf{B}_r$  represent the residual binarized matrix as the compensation. The final approximation of  $\mathbf{W}$  is  $\mathbf{W} \approx \alpha_o^* \mathbf{B}_o^* + \alpha_r^* \mathbf{B}_r^*$ .

**Non-Salient Part:** For the non-salient part (which is also symmetric Gaussian distribution), we find that significant information is retained in the non-salient part. To make the trade-off with bit and performance, we utilize a fine-grained grouping strategy called the Trisection search algorithm (See Alg. 2), whose aim is to find the optimal two break-point  $p_1^*, p_2^*$ . With these two break-points, we can segment the symmetric Gaussian distribution into three groups, which is sparse  $R_s[-m, -p_2^*] \cup [p_2^*, m]$ , intermediate  $R_i[-p_2^*, -p_1^*] \cup [p_1^*, p_2^*]$ , and dense region  $R_d[-p_1^*, p_1^*]$ . Then, we derive the quantization error:

$$\theta_{p_1^*, p_2^*}^2 = \|\mathbf{W}_s - \alpha_s \mathbf{B}_s\|^2 + \|\mathbf{W}_i - \alpha_i \mathbf{B}_i\|^2 + \|\mathbf{W}_d - \alpha_d \mathbf{B}_d\|^2, \quad (5)$$

$$\alpha_s = \frac{1}{n_s} \|\mathbf{W}_s\|_{l1}, \quad \alpha_i = \frac{1}{n_i} \|\mathbf{W}_i\|_{l1}, \quad \alpha_d = \frac{1}{n_d} \|\mathbf{W}_d\|_{l1} \quad (6)$$

where  $\mathbf{W}_s, \mathbf{W}_i, \mathbf{W}_d$  are the sums of absolute weight values in the sparse, intermediate, and dense regions.  $\mathbf{B}_s, \mathbf{B}_i, \mathbf{B}_d$  are the binarized weights for those regions. These three regions are binarized separately. This method introduces an additional 2 bits for group identification, which constitutes a minor portion of the overall bit count, while the majority of computing parameters remain at 1 bit.

**Average Bits.** In STBLLM, we introduce extra bits while pruning away the redundant or less important weights. The overhead of weight parameters is  $N_{\text{param}} = 2 \times r_{\text{salient}} + 1 \times (1 - r_{\text{salient}})$ . The additional hardware overhead is  $N_{\text{storing}} = 2 + \frac{1}{b_{\text{size}}}$ , where  $r_{\text{salient}}$  denotes the proportion of salient weights and  $b_{\text{size}}$  denotes the block size in OBC compensation, with 2 bits allocated for marking the division of non-salient weights. Under N:M binarization settings, where N and M are positive integers with  $N < M$ , we prune the model weights by retaining only a fraction (N/M) of the original weights. Consequently, the number of parameters in the pruned STBLLM model is  $N_{\text{stbllm}} = N_{\text{param}} \times \frac{N}{M}$ . This N:M binarization method allows for a significant reduction in model size.

## 4 Experiments

### 4.1 Implementation Details

**Experimental Setup.** Our proposed method, STBLLM, is implemented using the PyTorch [58] and Huggingface [59] libraries. Most experiments, excluding the LLaMA-1-65B model, can be evaluated on a single NVIDIA A800 GPU. For the LLaMA-1-65B model, we employ four NVIDIA A800 GPUs for evaluation. Notably, the LLaMA-1-7B and LLaMA-2-7B models can be evaluated using a single RTX 4090 GPU. Following BiLLM [23], our proposed STBLLM also eliminates the need for fine-tuning, offering an efficient post-training quantization framework.

**Datasets and Models.** We measure the perplexity for language generation tasks with Wikitext2 [60], C4 [61] and PTB [62], and accuracy for the zero-shot tasks including Winogrande [35], OBQA [36], Hellaswag [37], BoolQ [63], ARC [64] and RTE [65]. We conduct extensive experiments on LLaMA-1/2/3 [2, 32], OPT [33], and Mistral [34]. For perplexity evaluation in Table 2 and 4, we employ the C4 dataset as the calibration dataset and measure the perplexity on Wikitext2.

**Baseline.** Our primary baseline is BiLLM [23], which is a 1-bit PTQ framework for LLMs. We perform an N:M sparse pattern on pre-trained LLMs and then conduct the same procedure as BiLLM

Table 2: Perplexity comparison of PB-LLM and BiLLM on the LLaMA model family. The columns represent the perplexity results on the Wikitext2 for different model sizes. The average bit-width for each model is provided in the table. For more precise bit-width results, please refer to Table 1.

Method	Settings		LLaMA-1				LLaMA-2		LLaMA-3
	Block Size	W-Bits	7B	13B	30B	65B	7B	13B	8B
FullPrecision	-	16	5.68	5.09	4.1	3.53	5.47	4.88	6.10
RTN	-	1	1.7e5	1.4e6	1.5e4	6.5e4	1.6e5	4.8e4	2.7e6
GPTQ	128	1	2.7e5	1.1e5	6.7e4	2.5e4	1.2e5	9.4e3	5.7e4
PB-LLM	128	1.7	102.36	36.6	33.67	12.53	69.2	151.09	41.80
BiLLM	128	1.09	35.04	15.14	10.52	8.49	32.48	16.77	28.30
BiLLM	128	0.80 (6:8)	80.36	22.55	13.22	9.09	50.25	27.28	94.15
BiLLM	128	0.70 (5:8)	126.99	39.61	18.69	11.57	87.84	58.14	161.48
BiLLM	128	0.55 (4:8)	688.73	124.72	37.96	29.22	263.61	124.78	663.91
STBLLM	128	0.80 (6:8)	15.03	9.66	7.56	6.43	13.06	11.67	33.44
STBLLM	128	0.70 (5:8)	19.48	11.33	9.19	7.91	18.74	13.26	49.12
STBLLM	128	0.55 (4:8)	31.72	17.22	13.43	11.07	27.93	20.57	253.76

Table 3: Accuracies (%) for 7 zero-shot tasks from structured binarized LLaMA-1-13B, LLaMA-2-13B, and LLaMA-1-30B with BiLLM and STBLLM. We compare the performance under the same N:M setting to achieve sub-1-bit quantization.

Models	Method	Winogrande	OBQA	Hellaswag	Boolq	ARC-e	ARC-c	RTE	Mean
LLaMA-1-13B	FullPrecision	72.77	33.20	59.94	77.89	77.40	46.50	70.40	62.59
	BiLLM(6:8)	58.80	30.60	46.25	62.96	49.96	23.97	53.42	46.57
	BiLLM(4:8)	52.09	28.00	30.82	61.25	32.66	21.25	53.07	39.88
	STBLLM(6:8)	65.98	36.20	63.67	65.38	68.86	34.04	56.68	55.83
	STBLLM(4:8)	63.06	34.80	52.65	62.48	56.90	28.33	52.71	50.13
LLaMA-2-13B	FullPrecision	72.22	35.20	60.06	80.52	79.42	48.46	65.34	63.03
	BiLLM(6:8)	56.43	30.60	35.53	62.48	41.29	24.74	53.43	43.50
	BiLLM(4:8)	50.59	24.00	28.96	62.08	30.51	22.35	53.07	38.79
	STBLLM(6:8)	63.93	37.00	57.76	71.53	60.56	31.99	54.15	53.85
	STBLLM(4:8)	55.88	29.40	44.03	64.31	48.86	26.54	52.71	45.96
LLaMA-1-30B	FullPrecision	75.69	36.00	63.35	82.69	80.30	52.82	66.79	65.38
	BiLLM(6:8)	66.54	36.40	58.18	66.15	62.37	31.91	46.93	50.32
	BiLLM(4:8)	54.93	29.40	38.85	62.17	43.6	24.74	52.35	43.72
	STBLLM(6:8)	71.59	41.00	69.85	77.37	71.55	41.3	48.01	60.10
	STBLLM(4:8)	64.01	34.60	56.46	63.06	60.86	31.48	51.99	51.78

to report the results that are less than 1 bit (e.g. 0.8, 0.7, 0.55 bit). We conduct the N:M sparsity using Wanda [66] as the baseline, a gradient-free post-training pruning method. We compare the results of STBLLM with BiLLM under the same N:M settings. For more information on average bits under N:M settings, please refer to Table 1. Previous low-bit methods like PB-LLM [25], GTPQ [41] and vanilla RTN are also selected for comparison.

## 4.2 Main Results

**Comparison with PTQ methods.** We comprehensively compare the performance of different LLaMA families across various model sizes (7B-65B). For a fair comparison, we set the same block size to 128. As presented in Table 2, the model under RTN and GPTQ fails to retain the performance at 1-bit. PB-LLM has shown a satisfactory perplexity under 1.7 bit but deteriorates performance compared with BiLLM under 1.09 bit. To further compare the performance at sub-1-bit, we apply the same N:M setting to BiLLM and our proposed STBLLM. As shown in Figure 2, our proposed STBLLM achieves a better trade-off between bit-widths and perplexity across model sizes from 7B to 65B. STBLLM surpasses BiLLM by a large margin (688.73  $\rightarrow$  31.72) on LLaMA-1-7B, especially on the most extreme compression case, 4:8 structured binarization, which means setting half of the parameter to zero. It is also noteworthy that when the parameter size reaches 65B, our STBLLM, at 0.55 bit, achieves a perplexity of 11.07, surpassing that of PB-LLM (12.53) at 1.7 bit and that of BiLLM (11.57) at 0.7 bit. To our knowledge, our STBLLM is the first work that breaks the 1-bit barriers by further reducing the redundant weights in an N:M pattern. Moreover, we conduct further experiments on the OPT family from 1.3B to 30B and Mistral-7B at sub-1-bit PTQ settings. From Table 4, we observe the same trend as in LLaMA. Our proposed STBLLM performs significantly better than BiLLM across all models and all N:M structured binarization settings.



Table 4: Perplexity results on Wikitext2 datasets of OPT and Mistral models with BiLLM and STBLLM. For more precise bit-width results, please refer to Table 1.

Settings		OPT			Mistral	
Method	W-Bits	1.3B	2.7B	6.7B	30B	7B
BiLLM	0.80 (6:8)	51.62	23.03	15.82	15.82	72.29
BiLLM	0.70 (5:8)	69.15	30.62	20.58	20.58	82.84
BiLLM	0.55 (4:8)	106.99	55.28	79.68	79.68	189.73
STBLLM	0.80 (6:8)	29.84	17.02	12.79	12.80	27.31
STBLLM	0.70 (5:8)	33.01	20.82	14.38	14.38	25.64
STBLLM	0.55 (4:8)	45.11	30.34	18.80	18.80	70.14

**Zero-Shot Performance.** To conduct a more comprehensive evaluation of binary LLMs, we extend our experiments to 7 zero-shot datasets on LLaMA-1-13B, LLaMA-2-13B, and LLaMA-1-30B, each tested with FullPrecision, BiLLM(6:8), BiLLM(4:8), STBLLM(6:8), and STBLLM(4:8) methods. We mainly focus on the performance of these models under the sub-1-bit setting. Specifically, we compare the BiLLM and our STBLLM under 4:8 and 6:8 structured binarization settings. As illustrated in Table 3, we find that the performance drop in reduced precision methods is more pronounced in BiLLM methods compared to STBLLM methods, indicating that STBLLM methods are more robust alternatives when memory resources are constrained.

### 4.3 Ablation Studies

To better investigate our STBLLM, we provide detailed ablation studies showing the effectiveness of each component, the quantization strategy, and the allocation strategy. For more ablation studies, please refer to the Appendix B.

**Ablation for Metric.** Table 5 shows the impact of post-training pruning metrics (magnitude, Wanda [66], SparseGPT [29] and our SI) on STBLLM regarding LLaMA-1-7B and LLaMA-2-7B. During PTP, we employ the C4 dataset as the calibration dataset and report the perplexity on the Wikitext2 dataset. SparseGPT requires second-order information, which involves a massive computation burden. Similar to Wanda, our SI does not require gradient or second-order information. Our method achieves better performance among these metrics.

Table 5: Ablation for pruning metric.

Model	Magnitude	Wanda	SparseGPT	Ours (SI)
LLaMA-1-7B	4797.41	207.32	32.82	31.72
LLaMA-2-7B	2287.24	97.54	31.55	27.93

Table 6: Ablation for group size.

Model	64	128	256	512	1024
LLaMA-1-7B	29.58	31.72	33.97	41.29	146.46
LLaMA-2-7B	27.12	27.93	50.62	54.68	507.44

Table 7: Ablation for quantization strategy.

Models	BDS	NAQ
LLaMA-1-7B	80.35	15.03
LLaMA-2-7B	50.25	13.06

Table 8: Ablation study for allocation strategy.

Models	Uniform	Sin-shape	Ours
LLaMA-1-7B	80.36	67.78	15.03
LLaMA-2-7B	50.25	33.61	13.06

**Ablation for Quantization Strategy.** We conduct an ablation study on different quantization strategies. Comparing the perplexities of our Non-salient Aware Quantization (dubbed as NAQ) in STBLLM and Bell-shaped Distribution Splitting (dubbed as BDS) proposed in BiLLM [23] on both LLaMA-1-7B and LLaMA-2-7B models, results are shown in Table 7. The perplexity of NAQ changes a lot when moving from LLaMA-1-7B to LLaMA-2-7B, while our NAQ exhibits nearly identical perplexity in both models, significantly lower than that of BDS.

**Ablation for Allocation Strategy.** Table 8 presents an ablation study on different allocation strategies. We compare our method with Uniform and Sin-shaped allocation strategies. The Sin-shaped strategy assigns layer-wise sparsity following a sine wave pattern, where the initial layers have lower sparsity, and the latter layers have higher sparsity. The performance of Uniform and Sin-shaped strategies varies significantly across different models. In contrast, our strategy consistently achieves nearly identical perplexity across both models, significantly outperforming the other two allocation strategies.

**Ablation for Group Size.** Table 6 presents the results of our ablation study on the group size configuration. We evaluate the perplexity of LLaMA-1-7B and LLaMA-2-7B with group sizes of 64, 128, 256, and 512. Generally, as the group size increases, performance improves. However, this also results in higher computational and storage demands. To balance performance and resource consumption, we choose a group size of 128.

## 5 Conclusion

In this paper, we introduce a post-training framework with structured Binary LLMs, dubbed STBLLM, specifically designed for sub-1-bit quantization. Our findings reveal redundancy in binarized LLMs, highlighting the potential for further extreme compression. We present a novel gradient-free pruning metric, Standardized Importance (SI), for N:M structured pruning. For mixed N:M structured pruning, we develop a layer-wise binarization method to adaptively assign sparsity. Additionally, we utilize the Hessian matrix to partition weights into salient and non-salient categories. For non-salient weights, we propose Non-salient Aware Quantization, which identifies optimal breakpoints to create sparse, intermediate, and dense regions, each undergoing individual binarization. We validate the performance of STBLLM across LLaMA-1/2/3, OPT, and Mistral. Our results demonstrate that STBLLM achieves a superior trade-off at sub-1-bit settings. By pioneering LLM performance guarantees at an average bit rate of less than 1 bit, STBLLM showcases the potential of sub-1-bit LLMs and encourages further exploration in the extreme compression of LLMs.

**Limitation.** While STBLLM successfully breaks the barrier of 1-bit quantization with N:M sparsity, this paper focuses solely on sub-1-bit quantization and does not incorporate extensive compensatory techniques. As a result, we have not explored the performance of STBLLM at 1-bit and 2-bit quantization levels, which could further validate its effectiveness.

## References

- [1] Susan Zhang, Stephen Roller, Naman Goyal, Mikel Artetxe, Moya Chen, Shuohui Chen, Christopher Dewan, Mona Diab, Xian Li, Xi Victoria Lin, et al. Opt: Open pre-trained transformer language models. *arXiv preprint arXiv:2205.01068*, 2022. 1
- [2] Hugo Touvron, Thibaut Lavril, Gautier Izacard, Xavier Martinet, Marie-Anne Lachaux, Timothée Lacroix, Baptiste Rozière, Naman Goyal, Eric Hambro, Faisal Azhar, et al. Llama: Open and efficient foundation language models. *arXiv preprint*, 2023. 3, 7
- [3] Tom Brown, Benjamin Mann, Nick Ryder, Melanie Subbiah, Jared D Kaplan, Prafulla Dhariwal, Arvind Neelakantan, Pranav Shyam, Girish Sastry, Amanda Askell, et al. Language models are few-shot learners. *NeurIPS*, 2020. 1
- [4] Jason Wei, Xuezhi Wang, Dale Schuurmans, Maarten Bosma, Fei Xia, Ed Chi, Quoc V Le, Denny Zhou, et al. Chain-of-thought prompting elicits reasoning in large language models. *NeurIPS (NeurIPS)*, 35:24824–24837, 2022. 1
- [5] Jason Wei, Yi Tay, Rishi Bommasani, Colin Raffel, Barret Zoph, Sebastian Borgeaud, Dani Yogatama, Maarten Bosma, Denny Zhou, Donald Metzler, et al. Emergent abilities of large language models. *Transactions on Machine Learning Research*, 2022. 1
- [6] Sébastien Bubeck, Varun Chandrasekaran, Ronen Eldan, Johannes Gehrke, Eric Horvitz, Ece Kamar, Peter Lee, Yin Tat Lee, Yuanzhi Li, Scott Lundberg, et al. Sparks of artificial general intelligence: Early experiments with gpt-4. *arXiv preprint arXiv:2303.12712*, 2023. 1
- [7] Jue Wang, Yucheng Lu, Binhang Yuan, Beidi Chen, Percy Liang, Christopher De Sa, Christopher Re, and Ce Zhang. CocktailSGD: Fine-tuning foundation models over 500Mbps networks. In *ICML*. PMLR, 2023. 1
- [8] Zhenheng Tang, Yuxin Wang, Xin He, Longteng Zhang, Xinglin Pan, Qiang Wang, Rongfei Zeng, Kaiyong Zhao, Shaohuai Shi, Bingsheng He, et al. Fusionai: Decentralized training and deploying llms with massive consumer-level gpus. *arXiv preprint arXiv:2309.01172*, 2023. 1, 20
- [9] Tom B. Brown, Benjamin Mann, Nick Ryder and Melanie Subbiah, Jared Kaplan, Prafulla Dhariwal, Arvind Neelakantan, Pranav Shyam, Girish Sastry, Amanda Askell, Sandhini Agarwal, Ariel Herbert-Voss, Gretchen Krueger, Tom Henighan, Rewon Child, Aditya Ramesh, Daniel M, Ziegler, Jeffrey Wu, Clemens Winter, Christopher Hesse, Mark Chen, Eric Sigler, Mateusz Litwin, Scott Gray, Benjamin Chess, Jack Clark, Christopher Berner, Sam McCandlish, Alec Radford, Ilya Sutskever, and Dario Amodei. Language models are few-shot learners. *arXiv preprint, arXiv:2005.14165*, 2020. 1

- [10] Song Han, Huizi Mao, and William J. Dally. Deep compression: Compressing deep neural network with pruning, trained quantization and huffman coding. In Yoshua Bengio and Yann LeCun, editors, *ICLR*, 2016. 1
- [11] Fanxu Meng, Hao Cheng, Ke Li, Huixiang Luo, Xiaowei Guo, Guangming Lu, and Xing Sun. Pruning filter in filter. In *NIPS*, 2020. 1
- [12] Yuxian Gu, Li Dong, Furu Wei, and Minlie Huang. Knowledge distillation of large language models. *arXiv preprint*, 2023. 1
- [13] Saleh Ashkboos, Maximilian L. Croci, Marcelo Gennari do Nascimento, Torsten Hoefer, and James Hensman. SliceGPT: Compress large language models by deleting rows and columns. In *ICLR*, 2024. 1
- [14] Mohammad Rastegari, Vicente Ordonez, Joseph Redmon, and Ali Joseph. Xnor-net: Imagenet classification using binary convolutional neural networks. In *ECCV*, 2016. 2, 4, 5
- [15] Zechun Liu, Baoyuan Wu, Wenhan Luo, Xin Yang, Wei Liu, and Kwang-Ting Cheng. Bi-real net: Enhancing the performance of 1-bit cnns with improved representational capability and advanced training algorithm. In *ECCV*, 2018. 2, 4
- [16] Peisong Wang, Xiangyu He, Gang Li, Tianli Zhao, and Jian Cheng. Sparsity-inducing binarized neural networks. In *AAAI Conference on Artificial Intelligence*, 2020. 2, 4
- [17] Yikai Wang, Wen bing Huang, Yinpeng Dong, Fuchun Sun, and Anbang Yao. Compacting binary neural networks by sparse kernel selection. *2023 IEEE/CVF Conference on Computer Vision and Pattern Recognition (CVPR)*, pages 24374–24383, 2023. 2, 4
- [18] Yikai Wang, Yi Yang, Fuchun Sun, and Anbang Yao. Sub-bit neural networks: Learning to compress and accelerate binary neural networks. *2021 IEEE/CVF International Conference on Computer Vision (ICCV)*, pages 5340–5349, 2021. 2
- [19] Peisong Wang, Fanrong Li, Gang Li, and Jian Cheng. Extremely sparse networks via binary augmented pruning for fast image classification. *IEEE Transactions on Neural Networks and Learning Systems*, 34:4167–4180, 2021. 2, 4
- [20] Chen Liu, Ziqi Zhao, Sabine Süsstrunk, and Mathieu Salzmann. Robust binary models by pruning randomly-initialized networks. In Alice H. Oh, Alekh Agarwal, Danielle Belgrave, and Kyunghyun Cho, editors, *Advances in Neural Information Processing Systems*, 2022.
- [21] Yixing Li and Fengbo Ren. Bnn pruning: Pruning binary neural network guided by weight flipping frequency. *2020 21st International Symposium on Quality Electronic Design (ISQED)*, pages 306–311, 2020. 2, 4
- [22] Sri Aurobindo Munagala, Ameya Prabhu, and Anoop M. Namboodiri. Stq-nets: Unifying network binarization and structured pruning. In *British Machine Vision Conference*, 2020. 2, 4
- [23] Wei Huang, Yangdong Liu, Haotong Qin, Ying Li, Shiming Zhang, Xianglong Liu, Michele Magno, and Xiaojuan Qi. Billm: Pushing the limit of post-training quantization for llms. *ICML*, abs/2402.04291, 2024. 2, 4, 5, 6, 7, 9, 16
- [24] Yuzhuang Xu, Xu Han, Zonghan Yang, Shuo Wang, Qingfu Zhu, Zhiyuan Liu, Weidong Liu, and Wanxiang Che. Onebit: Towards extremely low-bit large language models. *arXiv preprint arXiv:2402.11295*, 2024. 4
- [25] Yuzhang Shang, Zhihang Yuan, Qiang Wu, and Zhen Dong. Pb-llm: Partially binarized large language models. *arXiv preprint*, 2023. 2, 4, 8
- [26] Itay Hubara, Brian Chmiel, Moshe Island, Ron Banner, Joseph Naor, and Daniel Soudry. Accelerated sparse neural training: A provable and efficient method to find n: m transposable masks. *NeurIPS (NeurIPS)*, 34:21099–21111, 2021. 2
- [27] Yuxin Zhang, Mingbao Lin, Zhihang Lin, Yiting Luo, Ke Li, Fei Chao, Yongjian Wu, and Rongrong Ji. Learning best combination for efficient n: M sparsity. In *NeurIPS (NeurIPS)*, 2022.

- [28] Aojun Zhou, Yukun Ma, Junnan Zhu, Jianbo Liu, Zhijie Zhang, Kun Yuan, Wenxiu Sun, and Hongsheng Li. Learning n: M fine-grained structured sparse neural networks from scratch. In *International Conference on Learning Representations (ICLR)*, 2021. 2
- [29] Elias Frantar and Dan Alistarh. Sparsegpt: massive language models can be accurately pruned in one-shot. In *Proceedings of the 40th International Conference on Machine Learning, ICML'23*. JMLR.org, 2023. 2, 4, 5, 6, 9
- [30] Mingjie Sun, Zhuang Liu, Anna Bair, and J Zico Kolter. A simple and effective pruning approach for large language models. In *ICLR*, 2024. 2, 4
- [31] Nvidia. Nvidia a100 tensor core gpu architecture, 2020. <https://www.nvidia.com/content/dam/enzz/Solutions/Data-Center/nvidia-ampere-architecture-whitepaper.pdf>. 2
- [32] Hugo Touvron, Louis Martin, Kevin Stone, Peter Albert, Amjad Almahairi, Yasmine Babaei, Nikolay Bashlykov, Soumya Batra, Prajwal Bhargava, Shruti Bhosale, et al. Llama 2: Open foundation and fine-tuned chat models. *arXiv preprint*, 2023. 3, 7
- [33] Susan Zhang, Stephen Roller, Naman Goyal, Mikel Artetxe, Moya Chen, Shuohui Chen, Christopher Dewan, Mona T. Diab, Xian Li, Xi Victoria Lin, Todor Mihaylov, Myle Ott, Sam Shleifer, Kurt Shuster, Daniel Simig, Punit Singh Koura, Anjali Sridhar, Tianlu Wang, and Luke Zettlemoyer. Opt: Open pre-trained transformer language models. *ArXiv*, abs/2205.01068, 2022. 3, 7
- [34] Albert Qiaochu Jiang, Alexandre Sablayrolles, Arthur Mensch, Chris Bamford, Devendra Singh Chaplot, Diego de Las Casas, Florian Bressand, Gianna Lengyel, Guillaume Lample, Lucile Saulnier, L'elio Renard Lavaud, Marie-Anne Lachaux, Pierre Stock, Teven Le Scao, Thibaut Lavril, Thomas Wang, Timothée Lacroix, and William El Sayed. Mistral 7b. *ArXiv*, abs/2310.06825, 2023. 3, 7
- [35] Keisuke Sakaguchi, Ronan Le Bras, Chandra Bhagavatula, and Yejin Choi. Winogrande: An adversarial winograd schema challenge at scale. *ACM*, 2021. 3, 7
- [36] Todor Mihaylov, Peter Clark, Tushar Khot, and Ashish Sabharwal. Can a suit of armor conduct electricity? a new dataset for open book question answering. In *EMNLP*, 2018. 3, 7
- [37] Rowan Zellers, Ari Holtzman, Yonatan Bisk, Ali Farhadi, and Yejin Choi. Hellaswag: Can a machine really finish your sentence? *ACL*, 2019. 3, 7
- [38] Zechun Liu, Barlas Oguz, Changsheng Zhao, Ernie Chang, Pierre Stock, Yashar Mehdad, Yangyang Shi, Raghuraman Krishnamoorthi, and Vikas Chandra. Llm-qat: Data-free quantization aware training for large language models. *arXiv preprint*, 2023. 4
- [39] Dayou Du, Yijia Zhang, Shijie Cao, Jiaqi Guo, Ting Cao, Xiaowen Chu, and Ningyi Xu. Bitdistiller: Unleashing the potential of sub-4-bit llms via self-distillation, 2024. 4
- [40] Hong Chen, Chengtao Lv, Liang Ding, Haotong Qin, Xiabin Zhou, Yifu Ding, Xuebo Liu, Min Zhang, Jinyang Guo, Xianglong Liu, et al. Db-llm: Accurate dual-binarization for efficient llms. *arXiv preprint arXiv:2402.11960*, 2024. 4
- [41] Elias Frantar, Saleh Ashkboos, Torsten Hoefler, and Dan Alistarh. Gptq: Accurate post-training quantization for generative pre-trained transformers. *arXiv preprint*, 2022. 4, 5, 6, 8
- [42] Jerry Chee, Yaohui Cai, Volodymyr Kuleshov, and Christopher De Sa. Quip: 2-bit quantization of large language models with guarantees. In *NeurIPS*, 2023. 4
- [43] Ji Lin, Jiaming Tang, Haotian Tang, Shang Yang, Xingyu Dang, and Song Han. Awq: Activation-aware weight quantization for llm compression and acceleration. *arXiv preprint*, 2023. 4, 5, 6
- [44] Changhun Lee, Jungyu Jin, Taesu Kim, Hyungjun Kim, and Eunhyeok Park. Owq: Lessons learned from activation outliers for weight quantization in large language models. *arXiv preprint arXiv:2306.02272*, 2023. 4

- [45] Tim Dettmers, Ruslan Svirschevski, Vage Egiazarian, Denis Kuznedelev, Elias Frantar, Saleh Ashkboos, Alexander Borzunov, Torsten Hoefer, and Dan Alistarh. Spqr: A sparse-quantized representation for near-lossless llm weight compression. *arXiv preprint*, 2023. 4
- [46] Hongyu Wang, Shuming Ma, Li Dong, Shaohan Huang, Huaijie Wang, Lingxiao Ma, Fan Yang, Ruiping Wang, Yi Wu, and Furu Wei. Bitnet: Scaling 1-bit transformers for large language models, 2023. 4, 20
- [47] Yoshua Bengio, Nicholas Léonard, and Aaron Courville. Estimating or propagating gradients through stochastic neurons for conditional computation. *arXiv preprint arXiv:1308.3432*, 2013. 4
- [48] Xinyin Ma, Gongfan Fang, and Xinchao Wang. Llm-pruner: On the structural pruning of large language models. In *NeurIPS*, 2023. 4
- [49] Saleh Ashkboos, Maximilian L. Croci, Marcelo Gennari do Nascimento, Torsten Hoefer, and James Hensman. SliceGPT: Compress large language models by deleting rows and columns. In *ICLR*, 2024. 4
- [50] Mengzhou Xia, Tianyu Gao, Zhiyuan Zeng, and Danqi Chen. Sheared llama: Accelerating language model pre-training via structured pruning. *ICLR*, 2024. 4
- [51] Yingtao Zhang, Haoli Bai, Haokun Lin, Jialin Zhao, Lu Hou, and Carlo Vittorio Cannistraci. Plug-and-play: An efficient post-training pruning method for large language models. In *ICLR*, 2024. 4, 5
- [52] Yongqi An, Xu Zhao, Tao Yu, Ming Tang, and Jinqiao Wang. Fluctuation-based adaptive structured pruning for large language models. In *AAAI*, 2023. 4
- [53] Hong Chen, Chengtao Lv, Liang Ding, Haotong Qin, Xiabin Zhou, Yifu Ding, Xuebo Liu, Min Zhang, Jinyang Guo, Xianglong Liu, and Dacheng Tao. Db-llm: Accurate dual-binarization for efficient llms. *ACL*, abs/2402.11960, 2024. 5, 6
- [54] Lu Yin, You Wu, Zhenyu Zhang, Cheng-Yu Hsieh, Yaqing Wang, Yiling Jia, Mykola Pechenizkiy, Yi Liang, Zhangyang Wang, and Shiwei Liu. Outlier weighed layerwise sparsity (OWL): A missing secret sauce for pruning LLMs to high sparsity, 2024. 5
- [55] Changhun Lee, Jungyu Jin, Taesu Kim, Hyungjun Kim, and Eunhyeok Park. Owq: Outlier-aware weight quantization for efficient fine-tuning and inference of large language models. In *AAAI*, 2023. 5
- [56] Wei Sun, Aojun Zhou, Sander Stuijk, Rob G. J. Wijnhoven, Andrew Nelson, Hongsheng Li, and Henk Corporaal. Dominosearch: Find layer-wise fine-grained n:m sparse schemes from dense neural networks. In *Thirty-Fifth Conference on Neural Information Processing Systems*, 2021. 6
- [57] Wenqi Shao, Mengzhao Chen, Zhaoyang Zhang, Peng Xu, Lirui Zhao, Zhiqian Li, Kaipeng Zhang, Peng Gao, Yu Qiao, and Ping Luo. Omniquant: Omnidirectionally calibrated quantization for large language models. In *ICLR2024 Spotlight*, 2023. 6
- [58] Adam Paszke, Sam Gross, Francisco Massa, Adam Lerer, James Bradbury, Gregory Chanan, Trevor Killeen, Zeming Lin, Natalia Gimelshein, Luca Antiga, et al. Pytorch: An imperative style, high-performance deep learning library. *NIPS*, 2019. 7
- [59] Thomas Wolf, Lysandre Debut, Victor Sanh, Julien Chaumond, Clement Delangue, Anthony Moi, Pierric Cistac, Tim Rault, Rémi Louf, Morgan Funtowicz, et al. Huggingface’s transformers: State-of-the-art natural language processing. *arXiv preprint arXiv:1910.03771*, 2019. 7
- [60] Stephen Merity, Caiming Xiong, James Bradbury, and Richard Socher. Pointer sentinel mixture models, 2016. 7
- [61] Colin Raffel, Noam Shazeer, Adam Roberts, Katherine Lee, Sharan Narang, Michael Matena, Yanqi Zhou, Wei Li, and Peter J. Liu. Exploring the limits of transfer learning with a unified text-to-text transformer. *arXiv e-prints*, 2019. 7



- [62] Mitchell P. Marcus, Beatrice Santorini, and Mary Ann Marcinkiewicz. Building a large annotated corpus of English: The Penn Treebank. *Computational Linguistics*, 19(2):313–330, 1993. 7
- [63] Christopher Clark, Kenton Lee, Ming-Wei Chang, Tom Kwiatkowski, Michael Collins, and Kristina Toutanova. Boolq: Exploring the surprising difficulty of natural yes/no questions, 2019. 7
- [64] Peter Clark, Isaac Cowhey, Oren Etzioni, Tushar Khot, Ashish Sabharwal, Carissa Schoenick, and Oyvind Tafjord. Think you have solved question answering? try arc, the ai2 reasoning challenge. *arXiv preprint*, 2018. 7
- [65] Tuhin Chakrabarty, Debanjan Ghosh, Adam Poliak, and Smaranda Muresan. Figurative language in recognizing textual entailment. *ArXiv*, abs/2106.01195, 2021. 7
- [66] Mingjie Sun, Zhuang Liu, Anna Bair, and J. Zico Kolter. A simple and effective pruning approach for large language models. In *ICLR*, 2024. 8, 9
- [67] Lei Wang, Lingxiao Ma, Shijie Cao, Quanlu Zhang, Jilong Xue, Yining Shi, Ningxin Zheng, Ziming Miao, Fan Yang, Ting Cao, Yuqing Yang, and Mao Yang. Ladder: Enabling efficient low-precision deep learning computing through hardware-aware tensor transformation. In *USENIX Symposium on Operating Systems Design and Implementation*, 2024. 20
- [68] Georgi Gerganov. llama.cpp: a c/c++ port of facebook ai’s llama language model. <https://github.com/ggerganov/llama.cpp>, 2023. 20
- [69] Brendan McMahan, Eider Moore, Daniel Ramage, Seth Hampson, and Blaise Agüera y Arcas. Communication-efficient learning of deep networks from decentralized data. In *AISTATS*, 2017. 20
- [70] Peter Kairouz et al. Advances and open problems in federated learning, 2021. 20
- [71] Zhenheng Tang, Yonggang Zhang, Shaohuai Shi, Xinmei Tian, Tongliang Liu, Bo Han, and Xiaowen Chu. Fedimpro: Measuring and improving client update in federated learning. In *ICLR*, 2024. 20
- [72] Zhenheng Tang, Yonggang Zhang, Shaohuai Shi, Xin He, Bo Han, and Xiaowen Chu. Virtual homogeneity learning: Defending against data heterogeneity in federated learning. In *Proceedings of the 39th International Conference on Machine Learning*, volume 162 of *Proceedings of Machine Learning Research*, pages 21111–21132. PMLR, 17–23 Jul 2022. 20
- [73] Binhang Yuan, Yongjun He, Jared Quincy Davis, Tianyi Zhang, Tri Dao, Beidi Chen, Percy Liang, Christopher Re, and Ce Zhang. Decentralized training of foundation models in heterogeneous environments. In *NeurIPS*. 20
- [74] Zhenheng Tang, Shaohuai Shi, Bo Li, and Xiaowen Chu. Gossipfl: A decentralized federated learning framework with sparsified and adaptive communication. *IEEE Transactions on Parallel and Distributed Systems*, pages 1–13, 2022.
- [75] Zichen Tang, Junlin Huang, Rudan Yan, Yuxin Wang, Zhenheng Tang, Shaohuai Shi, Amelie Chi Zhou, and Xiaowen Chu. Bandwidth-aware and overlap-weighted compression for communication-efficient federated learning. In *53rd International Conference on Parallel Processing*, Gotland, Sweden, 12–15 August 2024. 20
- [76] Peijie Dong, Lujun Li, Zimian Wei, Xin Niu, Zhiliang Tian, and Hengyue Pan. Emq: Evolving training-free proxies for automated mixed precision quantization. In *ICCV*, pages 17076–17086, 2023. 20
- [77] Peijie Dong, Lujun Li, and Zimian Wei. Diswot: Student architecture search for distillation without training. In *CVPR*, 2023.
- [78] Peijie Dong, Lujun Li, Zhenheng Tang, Xiang Liu, Xinglin Pan, Qiang Wang, and Xiaowen Chu. Pruner-zero: Evolving symbolic pruning metric from scratch for large language models. In *ICML*, 2024.

- [79] Zimian Zimian Wei, Lujun Li Li, Peijie Dong, Zheng Hui, Anggeng Li, Menglong Lu, Hengyue Pan, and Dongsheng Li. Auto-prox: Training-free vision transformer architecture search via automatic proxy discovery. In *AAAI*, 2024.
- [80] Lujun Li, Zimian Wei, Peijie Dong, Wenhan Luo, Wei Xue, Qifeng Liu, and Yike. Guo. Attnzero: Efficient attention discovery for vision transformers. In *ECCV*, 2024.
- [81] Lujun Li, Haosen Sun, Shiwen Li, Peijie Dong, Wenhan Luo, Wei Xue, Qifeng Liu, and Yike. Guo. Auto-gas: Automated proxy discovery for training-free generative architecture search. In *ECCV*, 2024. 20
- [82] Lujun Li and Zhe Jin. Shadow knowledge distillation: Bridging offline and online knowledge transfer. In *NeurIPS*, 2022. 20
- [83] Lujun Li, Peijie Dong, Anggeng Li, Zimian Wei, and Ya Yang. Kd-zero: Evolving knowledge distiller for any teacher-student pairs. *NeurIPS*, 2024.
- [84] Lujun Li. Self-regulated feature learning via teacher-free feature distillation. In *ECCV*, 2022.
- [85] Liu Xiaolong, Li Lujun, Li Chao, and Anbang Yao. Norm: Knowledge distillation via n-to-one representation matching. In *ICLR*, 2022.
- [86] Lujun Li, Yufan Bao, Peijie Dong, Chuanguang Yang, Anggeng Li, Wenhan Luo, Qifeng Liu, Wei Xue, and Yike Guo. Detkds: Knowledge distillation search for object detectors. In *ICML*, 2024. 20

## Appendix

### A STBLLM Implementation

Following BiLLM [23], STBLLM does not change the operations on salient weights. Instead, STBLLM mainly focuses on the non-salient weight. We present **NonSalientAwareQuant** and **Trisection** function in Alg. 2.

For **NonSalientAwareQuant** function, it aims to find two optimal break-points to partition the symmetric Gaussian distribution of non-salient weight. A naive approach for searching the break-point is using two nested loops, whose complexity is  $O(N^2)$ , where  $N$  denotes the length of the search space. To reduce the complexity to  $O(N)$ , we propose to utilize  $p_2 = \sigma \times p_1$  to locate the  $p_2$ . It is natural to assume that  $p_2 > p_1$  and we have  $\sigma > 1$ . In practice, we set the  $\sigma = 2$  and it works well.

For **Trisection** function, it aims to partition the symmetric Gaussian distribution presented in Figure 3(c) into three parts, which are Sparse, Intermediate, and Dense region. These three parts have no intersection and by uniting them together, we have all of the non-salient structured binarized weight.

---

#### Algorithm 2 STBLLM

---

<pre> func Salient (<math>\mathbf{W}, \mathbf{H}^c</math>) 1: <math>\mathbf{S} := \mathbf{W}^2 / [\mathbf{H}_{b:b+\beta; b:b+\beta}^c]^2</math> // salient matrix 2: <math>row_s\{\cdot\} := \text{topk}(\text{sum}(\text{abs}(\mathbf{S})).(\text{dim} = 0))</math> 3: <math>e = \text{inf}</math> // searching error 4: <math>n^* = 0</math> // optimal number of salient columns 5: <b>for</b> <math>i = 1, 2, \dots, \text{len}(row_s)</math> <b>do</b> 6:   <math>\mathbf{B}_1 := \text{binary}(\mathbf{W}_{:,j, j \in row_s[i]})</math> 7:   <math>\mathbf{B}_2 := \text{binary}(\mathbf{W}_{:,j, j \notin row_s[i]})</math> 8:   <b>if</b> <math>\ \mathbf{W} - (\mathbf{B}_1 \cup \mathbf{B}_2)\ ^2 &lt; e</math> <b>then</b> 9:     <math>e := \ \mathbf{W} - (\mathbf{B}_1 \cup \mathbf{B}_2)\ ^2</math> 10:    <math>n^* := i</math> 11:   <b>end if</b> 12: <b>end for</b> 13: <b>return</b> <math>row_s\{n^*\}</math>  func binary (<math>\mathbf{W}</math>) 1: <math>\alpha := \frac{\ \mathbf{W}\ _{\ell_1}}{m}</math> 2: <math>\mathbf{B} := \alpha \cdot \text{sign}(\mathbf{W})</math> 3: <b>return</b> <math>\mathbf{B}</math>  func Res_Approx (<math>\mathbf{W}</math>) 1: <math>\mathbf{B}_1 := \text{binary}(\mathbf{W})</math> 2: <math>\mathbf{R} := \mathbf{W} - \mathbf{B}_1</math> 3: <math>\mathbf{B}_2 := \text{binary}(\mathbf{R})</math> 4: <math>\mathbf{B} := \mathbf{B}_1 + \mathbf{B}_2</math> 5: <b>return</b> <math>\mathbf{B}</math> </pre>	<pre> func NonSalientAwareQuant (<math>\mathbf{W}</math>) 1: <math>e = \text{inf}</math> // searching error 2: <math>p_1^* = 0</math> // optimal break-point for trisection 3: <math>p_2^* = 0</math> // optimal break-point for trisection 4: <b>for</b> <math>i \in \text{np.linspace}(0.1, 0.9, 160)</math> <b>do</b> 5:   <math>p_1 := i \cdot \max(\text{abs}(\mathbf{W}))</math> 6:   <math>p_2 := \sigma \times p_1</math> 7:   <b>if</b> <math>p_2 &gt; 0.9 \times \max(\text{abs}(\mathbf{W}))</math> <b>then</b> 8:     <b>continue</b> 9:   <b>end if</b> 10:  <math>\mathbf{B}_1 := \text{binary}(\mathbf{W}_{ w_{i,j}  &gt; p_2})</math> 11:  <math>\mathbf{B}_2 := \text{binary}(\mathbf{W}_{ w_{i,j}  \leq p_2 \&amp;\&amp;  w_{i,j}  &gt; p_1})</math> 12:  <math>\mathbf{B}_3 := \text{binary}(\mathbf{W}_{ w_{i,j}  \leq p_1})</math> 13:  <b>if</b> <math>\ \mathbf{W} - (\mathbf{B}_1 + \mathbf{B}_2 + \mathbf{B}_3)\ ^2 &lt; e</math> <b>then</b> 14:    <math>e := \ \mathbf{W} - (\mathbf{B}_1 + \mathbf{B}_2 + \mathbf{B}_3)\ ^2</math> 15:    <math>p_1^* := p_1</math> 16:    <math>p_2^* := p_2</math> 17:  <b>end if</b> 18: <b>end for</b> 19: <b>return</b> <math>p_1^*, p_2^*</math>  func Trisection (<math>\mathbf{W}, p_1^*, p_2^*</math>) 1: <math>\tilde{\mathbf{B}}_2 := \text{binary}(\mathbf{W}_{ w_{i,j}  &gt; p_2^*})</math> 2: <math>\tilde{\mathbf{B}}_3 := \text{binary}(\mathbf{W}_{ w_{i,j}  \leq p_2^* \&amp;\&amp;  w_{i,j}  &gt; p_1^*})</math> 3: <math>\tilde{\mathbf{B}}_4 := \text{binary}(\mathbf{W}_{ w_{i,j}  \leq p_1^*})</math> 4: <b>return</b> <math>\tilde{\mathbf{B}}_2, \tilde{\mathbf{B}}_3, \tilde{\mathbf{B}}_4</math> </pre>
--	---

---

## B More Experimental Results

### B.1 Module Ablation Study

To evaluate the interdependent interaction between quantization and pruning within our STBLLM framework, we conduct a module ablation study. This study isolates the effects of quantization-only, pruning-only, and our combined method on the performance of the LLaMA-1-7B and LLaMA-2-7B models across the PTB, C4, and Wikitext2 datasets. The results are presented in Table 9.

The ablation results highlight the synergistic effect of combining quantization and pruning in our approach, significantly outperforming each method applied in isolation.

#### LLaMA-1-7B Analysis

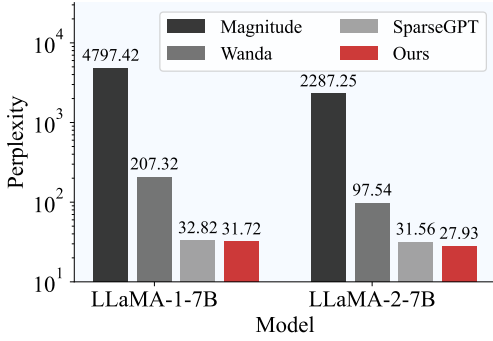


Figure 4: **Ablation study on post-training pruning metrics on STBLLM on LLaMA-1-7B and LLaMA-2-7B.** Our method achieves the best performance among these metrics.

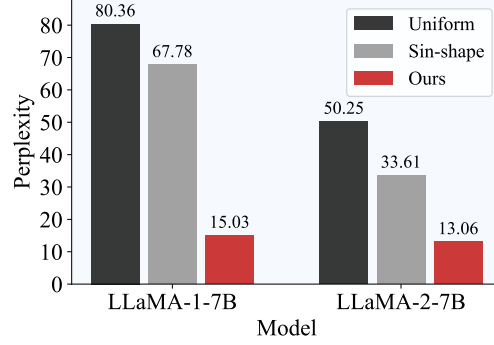


Figure 5: **Ablation study on allocation strategies on STBLLM on LLaMA-1-7B and LLaMA-2-7B.** Our strategy consistently achieves nearly identical perplexity across both models, significantly outperforming the other two allocation strategies

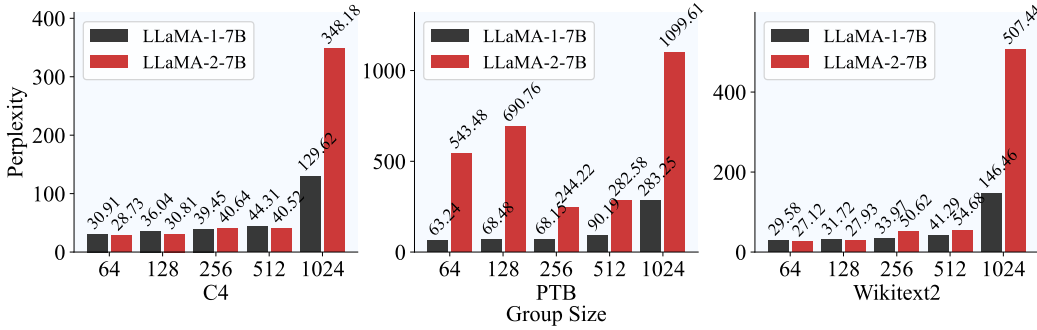


Figure 6: **Comparison across different sizes for LLaMA-1-7B and LLaMA-2-7B.**

- *PTB Dataset*: Our combined method achieves a score of 68.48, markedly higher than quantization-only (23.52) and pruning-only (14.24). This demonstrates the substantial performance gains achieved by leveraging the complementary strengths of both techniques.
- *C4 Dataset*: Our method scores 36.04, compared to 15.75 for quantization-only and 10.52 for pruning-only. The combined approach effectively mitigates the limitations of individual methods, resulting in superior performance.
- *Wikitext2 Dataset*: The score of 31.72 for our method far exceeds the results of quantization-only (12.29) and pruning-only (8.13), underscoring the enhanced model efficiency and accuracy through our integrated approach.

### LLaMA-2-7B Analysis

- *PTB Dataset*: Although quantization-only achieves an unusually high score of 2071.44, our combined method still significantly outperforms pruning-only (690.76 vs. 69.25). This suggests that while quantization might retain certain advantageous structures, the integration with pruning leads to a more balanced and robust model.
- *C4 Dataset*: The combined method's score of 30.81 surpasses quantization-only (14.62) and pruning-only (10.29), highlighting the effectiveness of our method in maintaining high performance across varying model versions.
- *Wikitext2 Dataset*: Our method's score of 27.93 is higher than both quantization-only (11.17) and pruning-only (7.85), further confirming the synergistic benefits of combining these techniques.

Table 9: Comparison of Quant-Only, Structure-Only, and ours across different datasets.

Dataset	LLaMA-1-7B			LLaMA-2-7B		
	Quant-Only	Structure-Only	Ours	Quant-Only	Structure-Only	Ours
PTB	23.52	14.24	68.48	2071.44	69.25	690.76
C4	15.75	10.52	36.04	14.62	10.29	30.81
Wikitext2	12.29	8.13	31.72	11.17	7.85	27.93

## B.2 Ablation Study of Calibration Dataset

Table 10 presents an ablation study comparing the performance of LLaMA-1-7B and LLaMA-2-7B models when trained on different calibration datasets: C4, PTB, and Wikitext2. The purpose of this experiment is to investigate how the choice of calibration dataset affects the models’ performance on various evaluation datasets.

In this study, both LLaMA-1-7B and LLaMA-2-7B models are trained on each of the three calibration datasets separately. The trained models are then evaluated on all three datasets, resulting in a 3x3 matrix of performance scores for each model.

The performance scores in the table likely represent some evaluation metric, such as perplexity or loss, where lower values indicate better performance. The diagonal values (e.g., C4 evaluated on C4) represent in-domain performance, while off-diagonal values represent out-of-domain performance.

By comparing the performance scores across different calibration datasets and evaluation datasets, researchers can gain insights into the generalization capabilities of the models and the impact of the calibration dataset on the models’ performance. This ablation study helps in understanding the sensitivity of the models to the choice of calibration data and can guide decisions on selecting the most suitable dataset for a given task or domain.

Table 10: Comparison of C4, PTB, and Wikitext2 across LLaMA-1-7B and LLaMA-2-7B

Dataset	LLaMA-1-7B			LLaMA-2-7B		
	C4	PTB	Wikitext2	C4	PTB	Wikitext2
C4	36.04	68.48	31.72	30.81	690.76	27.93
PTB	54.57	35.13	49.27	43.04	4569.03	40.94
Wikitext2	40.76	71.81	20.48	37.01	1970.76	20.60

## B.3 Ablation Study of Group Size

Table 11 and Figure 6 presents an ablation study that compares the performance of LLaMA-1-7B and LLaMA-2-7B models across different group sizes. The purpose of this experiment is to investigate how the choice of group size affects the models’ performance on various evaluation datasets.

In this study, both LLaMA-1-7B and LLaMA-2-7B models are trained with different group sizes: 64, 128, 256, 512, and 1024. The trained models are then evaluated on three datasets: C4, PTB, and Wikitext2.

The performance scores in the table likely represent some evaluation metric, such as perplexity or loss, where lower values indicate better performance. By comparing the performance scores across different group sizes and evaluation datasets, researchers can gain insights into the impact of group size on the models’ performance and generalization capabilities.

The results show that the performance of both models varies with the choice of group size. For LLaMA-1-7B, the best performance on C4 and Wikitext2 is achieved with a group size of 64, while for PTB, the best performance is obtained with a group size of 128. For LLaMA-2-7B, the best performance on C4 and Wikitext2 is also achieved with a group size of 64, while for PTB, the best performance is obtained with a group size of 256.

Interestingly, the performance of both models deteriorates significantly when the group size is increased to 1024, suggesting that excessively large group sizes may lead to overfitting or other training issues.

This ablation study helps in understanding the sensitivity of the models to the choice of group size and can guide decisions on selecting the most suitable group size for a given task or domain. It also highlights the importance of considering computational efficiency and memory constraints



when choosing the group size, as larger group sizes may require more resources during training and inference.

Table 11: Comparison across different sizes for LLaMA-1-7B and LLaMA-2-7B

Group Size	LLaMA-1-7B			LLaMA-2-7B		
	C4	PTB	Wikitext2	C4	PTB	Wikitext2
64	30.91	63.24	29.58	28.73	543.48	27.12
128	36.04	68.48	31.72	30.81	690.76	27.93
256	39.45	68.15	33.97	40.64	244.22	50.62
512	44.31	90.19	41.29	40.52	282.58	54.68
1024	129.62	283.25	146.46	348.18	1099.61	507.44

Table 12: Motivation vs Top Percentage

Top Percentage	Perplexity	Top Percentage	Perplexity	Top Percentage	Motivation
0.01	27.770422	0.02	30.168285	0.03	34.049734
0.04	36.191769	0.05	33.821476	0.06	36.452296
0.07	38.702617	0.08	39.169894	0.09	44.818825
0.10	54.451229	0.11	49.835159	0.12	71.762848
0.13	52.129317	0.14	52.568348	0.15	65.945448
0.16	62.712751	0.17	117.990227	0.18	138.912356

The provided Figure 1 and Table 12 present an experiment that investigates the relationship between the top Percentage of data and the corresponding perplexity scores in a language model. The purpose of this experiment is to understand how the choice of top Percentage affects the model’s performance and to determine an optimal threshold for data selection.

In this experiment, the language model is trained on a dataset, and the perplexity scores are calculated for different subsets of the data based on the top Percentages. The top Percentages range from 0.01 to 0.18, representing the proportion of the highest-quality or most relevant data points in the dataset.

Table 12 shows the perplexity scores for each top Percentage. Lower perplexity scores indicate better language model performance, as the model is better able to predict the next word in a sequence.

Figure 1 provides a visual representation of the relationship between the top Percentage and perplexity scores. It shows that the perplexity scores initially improve as the top Percentage increases, indicating that including more high-quality data points benefits the model’s performance. However, beyond a certain threshold (around 0.05 to 0.10), the perplexity scores start to deteriorate, suggesting that including lower-quality data points negatively impacts the model’s performance.

This experiment helps in understanding the importance of data selection in language modeling and highlights the need to find an optimal balance between data quality and quantity. The results suggest that focusing on a smaller subset of high-quality data points (e.g., top 5-10 Percentage) may lead to better model performance than including a larger but lower-quality dataset.

The insights gained from this experiment can guide data selection strategies and help in developing more efficient and effective language models. By carefully selecting the most relevant and high-quality data points, researchers can improve model performance while reducing computational costs associated with training on larger datasets.

### C Impact of Extreme Weight on the Hessian Matrix

The Hessian matrix  $H$  is defined as:  $H_{ij} = \frac{\partial^2 L}{\partial w_i \partial w_j}$ , where  $L$  is the loss function, and  $w_i$  and  $w_j$  are weights. If a weight  $w_k$  has extreme values, the corresponding elements in the Hessian matrix, particularly  $H_{kk}$ , will be significantly larger than others.

For instance, if  $w_1$  is an extreme value, the Hessian matrix might look like:

$$H = \begin{pmatrix} h_{11} & h_{12} & \cdots & h_{1n} \\ h_{21} & h_{22} & \cdots & h_{2n} \\ \vdots & \vdots & \ddots & \vdots \\ h_{n1} & h_{n2} & \cdots & h_{nn} \end{pmatrix}$$

Here,  $h_{11}$  is much larger than other elements. This disproportionate value significantly influences the Hessian’s eigenvalues, with at least one eigenvalue becoming very large. During optimization, methods like Newton’s method update weights using the inverse of the Hessian matrix:

$$\mathbf{w}_{\text{new}} = \mathbf{w} - \eta H^{-1} \nabla L(\mathbf{w}),$$

where  $\eta$  is the learning rate, and  $\nabla L(\mathbf{w})$  is the gradient. The presence of an extreme value in  $h_{11}$  causes the corresponding element in  $H^{-1}$  to be very small, affecting the step size in weight updates:

$$\Delta w_1 \approx -\eta \frac{\partial L}{\partial w_1} / h_{11},$$

$$\Delta w_2 \approx -\eta \frac{\partial L}{\partial w_2} / h_{22}.$$

Since  $h_{11}$  is large,  $\Delta w_1$  becomes small, indicating minimal adjustments for the extreme value weight, while  $\Delta w_2$  remains relatively larger for the normal weights.

## D Hardware Acceleration

When utilizing FP8 precision, it is observed that the model becomes memory-bound due to the limited reduction in memory bandwidth requirements relative to the decrease in computational complexity. To alleviate this, transitioning to 1-bit quantization proves advantageous, as it significantly reduces both computational overhead and memory footprint. This facilitates more efficient memory usage and faster data transfer rates. 1-bit quantization minimizes memory requirements and computational costs by reducing the precision of the weights to two possible states. This extreme form of quantization is particularly beneficial in resource-constrained environments, enhancing the deployability of large models on devices with limited hardware capabilities.

The adoption of semi-structured pruning techniques, specifically tailored for use with NVIDIA’s Ampere architecture, enables the employment of sparse tensor cores optimized for processing sparse matrices. By structuring the sparsity (e.g., N sparsity where N out of M weights are non-zero), these techniques effectively leverage the sparse tensor cores, which can lead to substantial improvements in processing speed and efficiency.

For 1-bit quantization, Ladder [67] has been released as BitBLAS, which can be integrated into existing DNN and LLM frameworks to enable efficient low-precision computing. For LLaMA-2-70B, Ladder accelerates BitNet 1.58 [46], achieving a 4.6× speedup over FP16. Besides GPUs, there is a framework called llama.cpp [68] that supports 1.5-bit quantization, namely BitNet [46], using CPUs. It achieves 198 tokens per second on just one CPU core.

## E Broader Impact

In the rapidly evolving landscape of artificial intelligence, the distributed training and federated learning of LLM has become increasingly important [69, 70, 8, 71, 72]. This shift is driven by the exponential growth in data volume and model complexity. However, the large communication overheads associated with LLMs pose significant challenges to the federated learning process. Model compression techniques have emerged as a solution, enabling more efficient training within federated learning frameworks [73–75]. STBLLM offers a novel approach to model compression by breaking the 1-bit quantization barrier through structured binarization. By utilizing N:M sparsity and introducing a new Standardized Importance (SI) metric for weight evaluation, STBLLM achieves extreme compression ratios while minimizing performance degradation. This makes it an ideal candidate for federated learning scenarios where communication efficiency and resource constraints are critical. The ability of STBLLM to maintain high performance at sub-1-bit precision enables the deployment of LLMs on resource-constrained devices, such as smartphones and IoT devices, which can be used in federated learning environments. This increased accessibility can democratize AI technologies, allowing more organizations and users to benefit from advanced language models without the need for extensive computational resources.

For future work, we plan to enhance STBLLM by integrating it with AutoML [76–81] and distillation methods [82–86]. AutoML techniques will automate the optimization of STBLLM architectures,

further improving their efficiency and performance. Distillation methods will be used to transfer knowledge from larger, high-precision models to STBLLM, enhancing its accuracy and robustness. These advancements will aim to further improve the efficiency and performance of LLMs in federated learning environments. By continuing to push the boundaries of model compression and efficiency, STBLLM paves the way for more sustainable and inclusive AI applications. However, it is crucial to address potential ethical concerns, such as bias in LLM outputs and the risk of misuse. Researchers and developers must collaborate with ethicists and policymakers to establish guidelines and safeguards that ensure the responsible deployment of these technologies.